

Neurobiology of Aging

Support vector machine learning and diffusion-derived structural networks predict amyloid quantity and cognition in adults with Down's syndrome

--Manuscript Draft--

Manuscript Number:	NBA-21-514R3
Article Type:	Regular Article
Section/Category:	Alzheimer's Disease & Other Dementias
Keywords:	Down's syndrome; Alzheimer's disease; dementia; MRI; diffusion MRI; Amyloid
Corresponding Author:	Stephanie S.G. Brown UNITED KINGDOM
First Author:	Stephanie S.G. Brown
Order of Authors:	Stephanie S.G. Brown Elijah Mak Isabel Clare Monika Grigorova Jessica Beresford-Webb Young T. Hong Tim D. Fryer Jonathan P. Coles Franklin I. Aigbirhio Dana Tudorascu Annie Cohen Bradley T. Christian Benjamin L. Handen William E. Klunk David K. Menon Peter J. Nestor Anthony J. Holland Shahid H. Zaman
Manuscript Region of Origin:	UNITED KINGDOM
Abstract:	<p>Down's syndrome results from trisomy of chromosome 21, a genetic change which also confers a probable one hundred percent risk for the development of Alzheimer's disease (AD) neuropathology in later life. We aimed to assess the effectiveness of diffusion-weighted imaging and connectomic modelling for predicting brain amyloid plaque burden, baseline cognition and longitudinal cognitive change using support vector regression. Ninety-five participants with Down's syndrome successfully completed a full Pittsburgh Compound B (PiB) PET-MR protocol and memory assessment at two timepoints. Our findings indicate that graph theory metrics of node degree and strength based on the structural connectome are effective predictors of global amyloid deposition. We also show that connection density of the structural network at baseline is a promising predictor of current cognitive performance. Directionality of effects were mainly significantly reductions in the white matter connectivity in relation to both PiB + status and above average longitudinal cognitive decline. Taken together, these results demonstrate the integral role of the white matter during neuropathological progression and the utility of machine learning methodology</p>

for non-invasively evaluating AD prognosis.



Stephanie S. G. Brown, Ph.D.
Research Associate
Department of Psychiatry

23rd February 2022

Covering letter:

Support vector machine learning and diffusion-derived structural networks predict amyloid quantity and cognition in adults with Down's syndrome

Dear Editor,

Please find attached the minor revision of our original research article entitled, '*Support vector machine learning and diffusion-derived structural networks predict amyloid quantity and cognition in adults with Down's syndrome*'. Utilizing a uniquely large participant sample of aging Down's syndrome individuals with Alzheimer's disease trajectory, we leverage a machine learning approach to predict both amyloid burden and longitudinal cognitive decline from the structural white matter network. Our work demonstrates how machine learning and the structural network are useful tools for predicting clinical outcomes.

The authors would like to thank the editor for the opportunity to amend and resubmit our manuscript. As per the reviewer comments, the sentence regarding data cleaning has been removed and Figure 2 has been amended to ensure a clearer edge-node representation.

The co-authors approve this manuscript and I can certify that this manuscript is not under review at any other publication. The work contained within this manuscript does not overlap with any other submissions or reports and conflicts are appropriately reported in the manuscript.

If you require any further information, please do not hesitate to contact me.

Yours sincerely,

A handwritten signature in cursive script that reads 'Stephanie S. G. Brown.'.

Stephanie S. G. Brown, Ph.D.

Credit Author Statement

Stephanie S. G. Brown: Conceptualization, methodology, formal analysis, investigation, writing – original draft

Elijah Mak: Resources

Isabel Clare: Project administration, data curation, validation

Monika Grigorova: Project administration

Jessica Beresford-Webb: Project administration

Madeline Walpert: Investigation

Elizabeth Jones: Project administration

Young T. Hong: Data curation, validation

Tim D. Fryer: Data curation, validation

Jonathan P. Coles: Data curation, validation

Franklin I. Aigbirhio: Data curation, validation

Dana Tudorascu: Data curation, validation

Annie Cohen: Funding acquisition, writing – review and editing

Bradley T. Christian: Funding acquisition, writing – review and editing

Benjamin L. Handen: Funding acquisition, writing – review and editing

William E. Klunk: Funding acquisition, writing – review and editing

David K. Menon: Funding acquisition, writing – review and editing

Peter J. Nestor: Funding acquisition, writing – review and editing

Anthony J. Holland: Supervision, funding acquisition

Shahid H. Zaman: Supervision, funding acquisition, writing – review and editing

Support vector machine learning and diffusion-derived structural networks predict amyloid quantity and cognition in adults with Down's syndrome

Stephanie S. G. Brown^{*1}, Elijah Mak¹, Isabel Clare¹, Monika Grigorova¹, Jessica Beresford-Webb¹, Madeline Walpert¹, Elizabeth Jones¹, Young T. Hong², Tim D. Fryer², Jonathan P. Coles³, Franklin I. Aigbirhio², Dana Tudorascu⁴, Annie Cohen⁴, Bradley T. Christian⁵, Benjamin L. Handen⁴, William E. Klunk⁴, David K. Menon³, Peter J. Nestor³, Anthony J. Holland¹, Shahid H. Zaman¹

¹ Cambridge Intellectual and Developmental Disabilities Research Group, Department of Psychiatry, University of Cambridge, United Kingdom.

² Department of Clinical Neurosciences, University of Cambridge, United Kingdom.

³ Department of Medicine, University of Cambridge, United Kingdom.

⁴ Department of Psychiatry, University of Pittsburgh, U.S.A.

⁵ Waisman Brain Imaging Laboratory, University of Wisconsin-Madison, U.S.A.

*Corresponding author email: sb2403@medschl.cam.ac.uk

Key words: Down's syndrome; Alzheimer's disease; dementia; MRI; diffusion MRI; amyloid

Highlights

- Down's syndrome confers a high risk for Alzheimer's neuropathology in later life
- We used diffusion-weighted imaging for support vector regression modelling
- Findings indicate that structural connectomics predict global amyloid deposition
- Connection density of the structural network is a predictor of cognitive performance

Abstract

Down's syndrome results from trisomy of chromosome 21, a genetic change which also confers a probable one hundred percent risk for the development of Alzheimer's disease (AD) neuropathology (amyloid plaque and neurofibrillary tangle formation) in later life. We aimed to assess the effectiveness of diffusion-weighted imaging and connectomic modelling for predicting brain amyloid plaque burden, baseline cognition and longitudinal cognitive change using support vector regression. Ninety-five participants with Down's syndrome successfully completed a full Pittsburgh Compound B (PiB) PET-MR protocol and memory assessment at two timepoints. Our findings indicate that graph theory metrics of node degree and strength based on the structural connectome are effective predictors of global amyloid deposition. We also show that connection density of the structural network at baseline is a promising predictor of current cognitive performance. Directionality of effects were mainly significant reductions in the white matter connectivity in relation to both PiB⁺ status and greater rate of cognitive decline. Taken together, these results demonstrate the integral role of the white matter during neuropathological progression and the utility of machine learning methodology for non-invasively evaluating AD prognosis.

Introduction

The brain is a complex, topological network, disruption and degeneration of which can result in profound cognitive and behavioural change. The foundation of structural brain connectivity is the white matter, which is comprised of the myelinated axonal projections of neurones (Bastin, Munoz Maniega et al. 2010). Inherently, the white matter of the brain provides integration and assimilation of complex biological functions dictated by specialised grey matter. Moreover, the role of white matter as a spreading mechanism for prion-like neurodegenerative proteins has been well-established (Polymenidou and Cleveland 2012, Rosen, Fritz et al. 2012, Costanzo and Zurzolo 2013). When organised into a connectomic approach, whereby robust reconstructions of white matter tracts are grouped into edge- and node-based networks, structural connectivity can be considered as a biological system of interconnected cortical and subcortical regions (Smith, Tournier et al. 2015). The structural connectome enables a more nuanced approach to mapping white matter than summary measures of microstructure diffusion anisotropy, which is a commonly used technique but one which may not leverage to the best advantage the full data range from diffusion-weighted imaging (Kaestner, Balachandra et al. 2020). Application of network and graph theories, which model and extract discrete mathematical characteristics from the system, allows for effective dimensionality reduction of information-dense neuroimaging data and provides uniformity for successful delineation of pathology (Rubinov and Sporns 2010). Such modelling of brain data may rely upon a multitude of acquisition types, including functional (Chang, Hsu et al. 2020), metabolic (Huang, Hsu et al. 2020), structural (Morgan, Seidlitz et al. 2019) and diffusion-weighted networks (Lin, Lin et al. 2019, Kuang, Gao et al. 2020).

The white matter is of particular pathological importance in the development, progression and seeding of neurotoxic proteins in Alzheimer's disease (AD) (Bloom 2014, Fornari, Schafer et al. 2019). In addition, white matter exhibits increased susceptibility to MRI

hyperintensities in tandem with amyloid accumulation (Graff-Radford, Arenaza-Urquijo et al. 2019, Moscoso, Rey-Bretal et al. 2020) and genetic predisposition for AD in human clinical populations (Lee, Viqar et al. 2016). For this reason, we hypothesised that a white matter network-based approach when evaluating brain function may be advantageous in the prediction of disease advancement. The study of AD in people with Down's syndrome (DS) across the age of risk for AD offers a unique opportunity to characterise pre-clinical pathological developments. This is particularly challenging when studying sporadic AD and therefore the early stages of neurodegeneration still remain under-researched. In DS, it is likely that 100% of individuals over the age of 40 years will exhibit AD neuropathology of amyloid accumulation and neurofibrillary tangle formation, despite AD penetrance over the lifespan not being complete for persons with DS (Wiseman, Al-Janabi et al. 2015). This predictable development of AD in aging persons with DS is driven by trisomy of chromosome 21, which contains multiple genes found to contribute to AD pathogenesis. A critical genetic change is the triplication of the *amyloid precursor protein* (APP) gene located on chromosome 21, the cleavage product of which is beta-amyloid (A β). This leads to the upregulation of misfolded accumulations of A β in the brain from as early as adolescence (Head, Helman et al. 2018). Indeed, having DS as a result of partial trisomy of chromosome 21 and no triplication of APP does not result in AD (Prasher, Farrer et al. 1998, Korbel, Tirosh-Wagner et al. 2009). As put forward by the amyloid cascade hypothesis amyloid deposition in the brain is hypothesised to be an early AD-related change, and a subsequent "trigger" for further pathogenic mechanisms, such as hyperphosphorylated tau-mediated microtubule disruption (Bloom 2014). Being able to measure this early A β accumulation is therefore critical to the advancement of clinical research and a key target for potential therapeutic modulation.

As the degree of structural connectivity has previously been linked with the prion-like propagation of A β in sporadic AD (Weickenmeier, Kuhl et al. 2018), the present study aimed to examine the relationship between the structural network characteristics, A β deposition and the outward manifestation of neuropathology, i.e. cognitive decline, in aging people with DS. In particular, we aimed to exploratorily assess the predictive power of the structural network, hypothesising that, given the integral role of white matter connectivity in both A β pathogenesis and cognition, alterations in the network may accurately forecast the degree of amyloid deposition and deterioration in working memory. The emerging role for machine learning in neuroscience has exhibited promising results for characterisation of disease state and prediction of continuous pathological outcomes (Zacharaki, Wang et al. 2009, Kassraian-Fard, Matthis et al. 2016), and we therefore developed and validated the performance of supervised support vector regression models in predicting both amyloid burden and longitudinal change in memory performance. The aims of this study were to demonstrate the utility of the structural network as a non-invasive biomarker for AD neuropathology and secondarily; to identify, on an anatomical level, the most statistically powerful brain regions for prediction and thereby, identify areas of the white matter most susceptible to alteration by AD development. We hypothesised that the white matter connectome may be an effective and non-invasive predictor of both cognitive decline and amyloid burden in DS.

Methods

Participant recruitment

Ninety-five Down's syndrome participants were recruited and successfully completed both an MRI and PiB-PET protocol across four study sites at University of Cambridge (n = 15), University of Pittsburgh (n = 34), University of Wisconsin-Madison (n = 38) and Barrow Neurological Institute (n = 8). All data was collected between 2017 and 2020. The inclusion criteria were as follows: Trisomy 21 confirmed by genotype, age above 25 years, baseline 'mental age' of 3 years or greater on either the Stanford Binet V or Peabody Picture Vocabulary Test, a reliable caregiver who was capable of providing correct information about the participants clinical symptoms and history, co-operation with protocol procedures. Participants were also assessed for potential exclusion criteria, which included: significant disease or unstable medical condition that could affect neuropsychological testing and contraindication for MRI scanning. All participants gave fully informed consent or assent and the study was approved by the appropriate regional ethics committees. Clinical diagnosis status for dementia or mild cognitive impairment (MCI) was decided at consensus diagnosis meetings at each research visit. The four diagnostic categories used were: "No MCI, no dementia", "MCI", "Dementia" and "Unable to determine". At least three clinicians experienced in the diagnosis of AD in DS were present at each meeting. They were given information about each participant's physical and mental health history, medications, age, IQ and any significant life events. Longitudinal change in the following scores was used to determine cognitive and functional decline: WISC Block Design (Wechsler 2003), Beery Visual-Motor Integration (Beery K.E. 1989), the NEPSY- Second Edition Word Generation Semantic Fluency subtest (Korkman M. 2007), Down Syndrome Mental Status Examination (Haxby 1989), The Dementia Questionnaire for People with Learning Disabilities (Evenhuis 2007), National Task Group Early Detection Screen for Dementia (Esralew 2013), Reiss Screen for Maladaptive Behavior (S. 1994).

Neuropsychological testing

The Cued Recall task was completed by 90 Down's syndrome participants at baseline, with 76 of these participants also completing the task 16 months after scanning. The Cued Recall Test measures episodic memory. The present test was modified from the version developed for the typical population (Buschke 1984). Three cards with four pictures per card were presented for learning, one card at a time. During the training phase, participants are given a unique category cue and were asked to point to and name the relevant picture. After naming each picture on the card, the card was removed, and the participants were asked to recall the pictures. This was repeated for all three cards, three trials per card. During the test phase, the participants were asked to recall all the pictures (Free Recall score). If they were not able to name all pictures spontaneously, they are given cues for the remaining items (Cued Recall score). Any intrusions were also recorded, and the full procedure was repeated three times. The Total Recall score is derived by summing all items recalled during Free Recall and Cued Recall and subtracting all intrusions.

Neuroimage acquisition

At the Cambridge site, a 3T GE Signa PET-MR system was used for all neuroimage data acquisition. University of Pittsburgh and University of Wisconsin-Madison PET data were

acquired on Siemens ECAT HR+ scanners and MRI data were acquired on a 3T SIGNA 750 (University of Wisconsin-Madison) or a Siemens 3T Magnetom Trio (University of Pittsburgh). Barrow Neurological Institute data were acquired using a Discovery 710 PET/CT scanner and a Discovery 3T MR750 MRI scanner. For all sites, MRI and PET data were acquired at the same study visit for all participants.

Fast spoiled gradient echo (FSPGR) T₁-weighted anatomical data was acquired for 61 of the participants with 1.05 x 1.05 x 1.2mm³ voxel size. Repetition time (TR) was 7.348 ms, echo time (TE) was 3.036 ms, the flip angle was 11 degrees and matrix size was 256 x 556 x 196 mm. Magnetization prepared rapid gradient echo (MPRAGE) T₁-weighted anatomical data was acquired for 34 participants with 1.05 x 1.05 x 1.2mm³ voxel size. TR was 2300 ms, TE was 2.95 ms and the flip angle was 9 degrees. Matrix size was 176 x 240 x 256 mm.

Diffusion data was acquired for all 95 participants in the axial plane with 48 diffusion directions. Field of view (FOV) was 23.2 cm with 2.0 mm slice thickness. Optimized TE was minimum and TR was 15707.0 ms with real time field adjustment. Voxel size was 0.9 x 0.9 mm², matrix size was 256 x 256 x 80 mm, b value = 1000 and a single b₀ scan was acquired. Phase encoding was in the anterior-posterior direction.

Structural MRI processing

T₁-weighted structural data were pre-processed using the FreeSurfer v6.0 'recon-all' pipeline (<https://surfer.nmr.mgh.harvard.edu/fswiki/recon-all>), which carried out the following steps: intensity correction, transform to MNI template, intensity normalization, skull strip, subcortical segmentation, neck remove, subcortical labelling, segmentation statistics, a second intensity correction using brain only (after skull strip), white matter segmentation, subcortical mass creation, brain surface creation, surface inflation, automatic topology fixer, cortical thickness/pial surfaces, cortical ribbon mask, spherical inflation of the brain surface, ipsilateral surface registration, contralateral surface registration, resampling of the average atlas curvature to subject, cortical parcellation and creation of summary table for parcellation statistics.

Diffusion MRI processing

Diffusion-weighted data were denoised using MRTrix3 (Tournier, Smith et al. 2019). Whole brain masking was carried out using the co-registered brain mask output from FreeSurfer structural image processing. Anatomical parcellated and segmented structural images from the T₁ pipeline were co-registered to diffusion space (B₀ image) using Statistical Parametric Mapping software (SPM12) with nearest neighbour interpolation to preserve labels. B₁ field inhomogeneity correction was applied to the diffusion images using the MRTrix3 command 'dwibiascorrect' (Tournier, Smith et al. 2019), and the fibre orientation distribution images (FODs) were created using constrained super-resolved spherical deconvolution (Tournier, Calamante et al. 2007, Dell'Acqua and Tournier 2018). The MRTrix command '5ttgen' was used to produce a five tissue-type segmentation image that was used for anatomically constrained tractography and a segmented mask image was created for use as tractography seeding localisation at the grey-white matter interface (Tournier, Smith et al. 2019). The FODs were subsequently used as the basis for creation of whole brain tractograms (Tournier

J.D. 2010). Five million seeds were used, with default parameters of 0.1mm x voxel size for individual step size for probabilistic building of streamlines. FOD amplitude cut-off was 0.05 and the maximum angle between successive steps was $90^\circ \times \text{step size} \times \text{voxel size}$. Spherical deconvolution informed filtering of the tractograms was then carried out ('SIFT2') (Smith, Tournier et al. 2015), to remove streamlines unlikely to be relevant to underlying ground truth anatomy. MRTrix was used to create a structural connectome based on connection density between T_1 structural nodes (Tournier, Smith et al. 2019). All processed structural data was visually assessed for quality assurance.

Graph theory metrics were extracted from the connectomes using Brain Connectivity Toolbox (Rubinov and Sporns 2010). For all 84 regional brain nodes, node degree (number of links connected to the node) and node strength (sum of connection density weights connected to the node) was calculated. Additionally, global efficiency (average inverse shortest path length in the network) was calculated for each participant.

Pittsburgh Compound B (PiB) PET image processing

PiB-PET images were acquired over a range of time that included 50-70 minutes post injection. Scans were binned into 5-minute intervals spanning this range and were inspected for interframe motion and, if necessary, corrected using PMOD. Motion-corrected frames were averaged to produce a single 50-70 minute mean image. T_1 -weighted MR scans (acquisition described in *Neuroimage acquisition*) were aligned to ACPC orientation and the mean single frame PET image aligned using PMOD. The T_1 image was used as input to FreeSurfer 5.3 which was used to parcellate the images into the standard FreeSurfer regions with the following exception: the FreeSurfer striatal region was replaced by the striatal region from the Imperial College London Clinical Imaging Centre (CIC) atlas (Tziortzi, Searle et al. 2011) which is more detailed in its parcellation. This was accomplished by the warping the CIC atlas into internal FreeSurfer space. For each participant, images were visually inspected and quality checked to ensure correct alignment. The warped atlas was then warped into each subject's space using the subject transformation generated during the processing of each subject. Standardized uptake value ratios (SUVR) were generated for each standard region by firstly performing a volume-weighted average of activity concentration in the constituent FreeSurfer/CIC regions and secondly normalizing by the cerebellar gray-matter activity.

Resolution compensation (partial volume correction, PVC) was performed using the Geometric Transfer Matrix (GTM) method (Rousset, Ma et al. 1998). Application of GTM requires an estimate of each scanner's point-spread function. These were obtained by an analysis of Hoffman Brain Phantom data that each site supplied as part of site-qualification for this study. Regional PiB⁺ and regional PiB⁻ were defined with GTM SUVR cut-offs as described by Zammit *et al* (2020, 2021) (Zammit, Laymon et al. 2020, Zammit, Tudorascu et al. 2021), derived from longitudinal analysis in DS that distinguished early accumulators from non-accumulators. As triplication of the APP gene leads to a striatal-dominant pattern of amyloid accumulation, the striatum was also used as region of interest for PiB binding; the template for amyloid burden and tissue segmentation for DS is described in Lao *et al* (2020) (Lao, Handen et al. 2019). The thresholds were 1.885 for the anterior cingulate, 1.398 for the striatum, 1.784 for the superior frontal, 1.777 for the orbitofrontal, 1.369 for the

insula, 1.57 for the lateral temporal, 1.796 for the parietal, 1.811 for the posterior cingulate, 1.946 for the precuneus and 1.731 globally. Global SUVR was defined as an average of the other regions of interest. An ROI in the cerebellar grey matter drawn in native space was used as a reference region (Lao, Handen et al. 2019). Individuals exceeding the cut-off SUVR measurement in any of these regions were defined as PiB⁺.

Rank-based feature selection and support vector machine regression modelling

Structural connectome matrix data (size: 84x84, upper triangle) was vectorised, and vectorised data was concatenated. Vectors of graph theory metrics were concatenated, and were feature selected separately to connectome data. Rank-based feature selection was carried out on ten PiB⁺ and ten PiB⁻ individuals in the dataset who were then excluded from further analysis. For the assessment of global amyloid- β as an outcome variable, data was grouped into regional PiB⁺ and regional PiB⁻ participants and student's two-tailed t-tests assuming equal variance were performed on each network feature and graph metric. P values were then ranked, and $p < 0.01$ graph metric features and $p < 0.01$ structural connectome features were preserved for further analysis. For the assessment of cognitive performance, longitudinal change (*Longitudinal change = Month 16 total recall – Baseline total recall*) in total cued recall was binarized into below mean and above mean change. Mean longitudinal cognitive change of the whole sample was -6.7 points on the Cued Recall Task total score. Two-tailed t-tests were carried out between ten individuals below average cognitive change and ten individuals above average cognitive change and p values were ranked. The 20 participants used for feature selection were then excluded from subsequent SVM modelling. For the graph metric and structural connectome features, $p < 0.01$ were preserved for further analysis.

Linear kernel-based support vector machine (SVM) regression models, fully described by Drucker *et al*, 1997 (Drucker 1997), were trained and evaluated for the selected network features, using global PiB SUVR, cognitive performance and longitudinal cognitive change as measured by the Cued Recall Task (see section: *Neuropsychological testing*) as outcomes. Models were developed and implemented using the Regression Learner Toolbox in MATLAB (R2019b) (<https://www.mathworks.com/help/stats/regression-learner-app.html>). Model evaluation utilized root mean square error (RMSE), R^2 , mean square error (MSE) and mean absolute error (MAE) as performance metrics. These metrics for the trained model may be interpreted as follows: RMSE values have the same unit as the response variable, with smaller values indicating smaller error (Chai 2014). R^2 is the coefficient of determination, with a value smaller than 1, it compares the trained model with a model where the response is constant, therefore if the trained model performs worse than the constant model, R^2 will be negative; a positive R^2 indicates the model performs more favourably than chance (Glantz 1990). MSE is the square of the RMSE, where smaller values are favourable, and similarly MAE is the absolute error, which is always positive but less sensitive to outliers than the RMSE (Chai 2014).

For model validation, a k -fold cross validation approach was used, which minimizes the sampling bias that classically occurs with basic train/test data splitting and produces performance metrics based on the mean of partitioned repeated model tests. A standard of 5-folds was used, where each observation is randomly assigned into five approximately

equal groups with the training fold containing 4/5th of the data and the test fold containing the remaining 1/5th of the data, which allows for prioritisation of both accuracy and computational complexity (Xu and Goodacre 2018). As age is an important and known predictor of dementia pathology, age was included in all models and additionally assessed as a single predicting metric. All models were performed as a complete-case analysis (i.e. participants included had no missing datapoints).

Results

Participant demographics

Participant demographics for the complete sample are summarised in Table 1. Longitudinal change in total recall performance was nominally significant ($p = 0.04$) between the PiB⁺ and PiB⁻ groups, and total recall at baseline was also significantly different between groups ($p < 0.01$) indicating, as expected, a more overt cognitive decline was present in the individuals with positive PiB scans. Age was also significantly higher in the PiB⁺ group ($p < 0.01$). Between the PiB⁺ and PiB⁻ groups, sex was not significantly different ($p = 0.14$). Consensus diagnosis at baseline confirmed three PiB⁺ DS individuals with MCI, three with dementia and one unable to determine. One PiB⁻ participant was diagnosed with MCI and one was unable to determine. For the whole sample, age was significantly positively correlated with global PiB SUVR ($p < 0.001$) and negatively associated with total recall longitudinal change ($p < 0.01$) (fig.1).

Rank-based feature selection

Out of the full dataset, 1165 out of 7056 features of the structural network were selected by rank-based methods to be used in the SVM analysis ($p_{uncorr} < 0.01$) between the PiB⁺ and PiB⁻ groups. For the graph theory metrics, 22 out of 170 features were selected ($p_{uncorr} < 0.01$) using the PiB^{+/-} rank method. For the prediction of cognitive change, 22 out of 7056 features of the structural network were selected for inclusion in the SVM models, by ranking of p values between above mean and below mean longitudinal cognitive change ($p_{uncorr} < 0.01$). No features were selected for the cognitive measures from the graph theory metrics, as no features exhibited sufficiently significant between group differences ($p_{uncorr} < 0.01$).

Feature-selected network characteristics predictive of amyloid deposition, cognitive performance and cognitive decline

Selected features for the structural connectome predictive model for global brain amyloid deposition revealed that the features most significantly different in PiB⁺ DS individuals compared to PiB⁻ individuals included widespread limbic (amygdala and hippocampal complex), nucleus accumbens, frontal, temporal, occipital and cingulate white matter connectivity measures. Notably, the feature selection for the PiB SUVR models using the structural network data produced the most extensive number of significantly different regions of connectivity. In addition, the selected features of white matter connectivity were significantly lower in the PiB⁺ group compared to the PiB⁻. By contrast, the structural network feature-selected based on cognitive performance produced a lower number of significantly differing regions of connectivity, which were mainly focussed to the pallidum,

cingulate cortex, putamen and caudate. The majority of the selected features were significantly decreased regions of connectivity in the above average cognitive decline group compared to the below average cognitive decline group, however a small number of features exhibited between hemisphere increases in connection density (fig.2). Similarly, the selected graph theory metrics based on PiB^{+/-} significant differences were modest in number, with the strength and degree of connectivity at the limbic nodes (amygdala and hippocampal complex), the orbitofrontal cortex and nucleus accumbens exhibiting p values of less than 0.01. All features showed uniform decreases in node strength and degree of connectivity in the above average cognitive decline group (fig.3).

Support vector machine regression model performance

Five-fold cross-validation was performed for each model, thereby protecting against over-fitting via partitioning of the dataset. All model performance metrics are reported in Table 2. Linear regression SVMs carried out on the selected features of the structural network predicted amyloid deposition via PiB binding with an RMSE of 0.43 (SUVR) and an R² value of 0.15. The selected features of the structural network predicted baseline cognitive performance with a RMSE of 8.56 (total score on cued recall) and an R² value of 0.34, indicating that variation in the structural network is accounted for slightly more by cognitive performance than by amyloid deposition. The model predicting longitudinal cognitive change by the structural network was less effective, likely due to the network as measured at baseline being relatively poor at predicting month 16 functional cognition. The MAE for these models was 0.27 (PiB SUVR), 5.58 (recall baseline) and 7.10 (recall change), indicating with closeness of MAE to RMSE that model error was frequent but small.

The graph theory metrics as predictors of amyloid deposition produced the most effective model for PiB SUVR, with a RMSE of 0.40, an R² of 0.28 and a MAE of 0.26. A low MSE of 0.16, compared to the structural network predicted PiB SUVR model MSE of 0.19 is supportive of good model performance. For the cognitive score predictions, no graph theory metrics survived feature selection at the prescribed level of $p < 0.01$, and therefore no SVM models were produced for these measures.

Age-only predictive models for PiB SUVR and recall baseline performed more poorly than models that included the feature-selected graph theory and/or structural connectome data, based on the RMSE, R², MSE and MAE values. However, an age-only SVM model showed the most predictive power for estimating the longitudinal change in cognition, with an RMSE of 9.80, an R² of 0.17 and a MAE of 6.41. As with all predictive models of cognitive performance however, relatively high MSE scores indicate a larger margin of error. Comparatively, the predictive model of longitudinal cognitive change incorporating the structural network features had a slightly higher RMSE and lower R², which overall indicates that diffusion MRI measures acquired at baseline are not as effective as a simple age-only prediction for changes that occur 16 months post-scan.

Discussion

This is the first study to date to examine the white matter connectome in DS, and moreover is the most highly powered investigation to date into the power of the structural network

for predicting PET-measured neuropathological change and cognitive decline in a population with a likely 100% risk for AD pathogenesis. Our findings indicate that support vector regression models, using selected features of the structural connectome and graph theory metrics of node strength and degree, show promising performance when it comes to the prediction of brain amyloid deposition and cognitive performance. Rank-based feature selection from graph theory metrics did not however exhibit a favourable predictive ability for cognitive indices, suggesting that such network features may not be closely coupled to cognitive function. In addition, we highlight the regional importance of structural connectivity of a more widespread and extensive nature for amyloid deposition and a more limited network for cognitive decline. Interestingly, we also highlight the directional character of significant predictors in the models, showing the importance of pathology-related decline in connectivity and by contrast, minimal cross-hemispheric compensatory increases in the network connection density during the developmental processes of AD in DS.

The support vector regression models utilising the structural connectome as observed variables produced conservative RMSE values and R^2 estimations of effect size that explained a tolerable portion of variance in cognitive performance and amyloid deposition. The successful estimation of PiB binding in the brain by the structural connectome and node degree and strength indicates a mechanistic link between white matter connectivity and progressive amyloid plaque formation. Recent evidence has shown that in sporadic AD, lower levels of CSF A β -42, reflecting higher retention in the brain parenchyma, was significantly correlated with total volume of white matter hyperintensity (Weaver, Doeven et al. 2019). Similarly, in individuals with autosomal dominant AD, white matter hyperintensities were significantly more prevalent approximately six years prior to expected symptom onset, especially in the parietal and occipital lobes (Lee, Viqar et al. 2016). In contrast to tau burden, which has been reported to show no association with hyperintense signals in the white matter, white matter hyperintensities have been shown to exhibit a topographic pattern of amyloid-association in the frontal and parietal lobes in the non-demented elderly (Graff-Radford, Arenaza-Urquijo et al. 2019). Using the diffusion tensor model Powell *et al*, showed that in DS, white matter fractional anisotropy, which can be interpreted as a measure of microstructural order of the tissue, was reduced in conjunction with poorer cognitive performance (Powell, Caban-Holt et al. 2014). Additionally, the typically late myelinating pathways of the frontal regions were particularly affected, suggesting a role for developmental white matter myelination in subsequent neurodegenerative vulnerability (Powell, Caban-Holt et al. 2014, Fenoll, Pujol et al. 2017). Positive status for PiB binding has also shown to increase white matter damage in DS. Therefore, our findings provide further evidence that it is likely that amyloid accumulation may mechanistically exacerbate white matter abnormalities in the already atypical DS brain (Neale, Padilla et al. 2018).

Estimation of cognitive performance at baseline using the structural connectome by support vector regression yielded a promising model. A prediction error of within 8.56 points of change in total score in the cued recall task was achieved, within a data range of 75 points. This result suggests that this model would be more effective as a prediction tool for individuals with more pronounced cognitive decline. This may be due to a substantial degree of variability in network connectivity being attributable to individuals who exhibit

increased symptomology. Previous longitudinal findings have highlighted a sharp increase in $A\beta$, a phenomenon known to be detrimental to white matter integrity, that precedes the onset of clinical dementia and cognitive decline (Mak, Bickerton et al. 2019). Similarly, decreased fractional anisotropy and increased mean diffusivity have recently been highlighted as a correlate of poorer episodic memory in aging persons with DS (Bazydlo, Zammit et al. 2021). In addition, individuals with subjective cognitive decline without DS exhibit significantly lower microstructural order in the white matter in a widespread manner, which underscores the importance of white matter functionality in cognition (Ohlhauser, Parker et al. 2019). Rate and age of onset of cognitive decline is variable in DS-AD, despite almost universal prevalence of AD neuropathology in the fourth decade of life (Wiseman, Al-Janabi et al. 2015), indicating a complex balance of both potentially protective and pathological mechanisms. We show here the integral link with and predictive power of the white matter connectome for cognitive function.

The structural network and graph theory metrics, however, were a poor predictor of future cognitive performance as quantified by the cued recall task 16 months post-scan, and did not perform better than an age-only model. A plausible explanation for this discrepancy is that white matter assessment at baseline cannot accurately predict future changes, and there is a significant confound of existing (pre-morbid) and variable intellectual disability in DS, which cannot be effectively separated from AD-related cognitive decline. Graph theory-based network characteristics have previously been reported as a useful validation of trans-neuronal spread of hyperphosphorylated tau in AD, with strongly connected nodes exhibiting a higher burden of tauopathy (Cope, Rittman et al. 2018) and large-scale functional disconnection has been identified preclinically (Brier, Thomas et al. 2014). Our graph data extracted from the structural connectome however, despite showing group differences between above / below mean cognitive change, perform poorly in explaining variance in the degree of cognitive change. This suggests a limited association.

Our results highlight specific areas of regional significance for the effective prediction of both cognitive function at the time of scanning and brain amyloid deposition using the structural connectome and graph theory. Widespread limbic, frontal, temporal and occipital features of the structural network exhibit lower network connection density in association with increased amyloid burden, indicating that these reduced regions of connectivity are important for effective correlative prediction. Of the prominent selected features, the precentral gyrus is the site of the primary motor cortex (Catani 2019) and the lateral occipital cortex is a visual area mainly involved in object perception and recognition (Grill-Spector, Kourtzi et al. 2001). The isthmus of the cingulate is continuous with the parahippocampal gyrus and is thereby highly integrated with the temporal lobe (Zhu, Li et al. 2014), and the middle temporal cortex is a region important for the controlled retrieval of semantic and non-semantic memory (Davey, Thompson et al. 2016). The established significant role of the temporal lobe in AD pathology (Veitch, Weiner et al. 2019) and functionality of these regions strongly suggest that the dysconnectivity of the integration between motor, perception and memory cortices is pathologically significant. In sporadic AD, connectomic DWI analysis similarly revealed significant involvement of the middle temporal and motor regions in predicting AD progression using multivariate distance matrix regression, which is comparable to the white matter pathways highlighted as significant predictors in the present study for DS-AD (Ye, Mori et al. 2019). These common findings are

supportive of the white matter network as a promising and robust biomarker for disease advancement. Conversely, in addition to network disconnection, we also show a small role for apparent compensatory increases in network connectivity in the prediction of cognitive function from the structural connectome, whereas for PiB binding the directionality of predictive ability is uniformly towards decreased connection density in the network. These discrete cross-hemisphere regions of positive association between cognitive function and structural connectivity involved the superior frontal and precentral areas. This enhanced lateralised network integration of the frontal cortices suggest higher-level compensatory processes involving learning and memory functionality. Interestingly, these areas have been shown to be somewhat spared in the early DS-AD stages of development in longitudinal assessment (Mak, Bickerton et al. 2019) and therefore predictive importance may arise from the ability to increase connectivity due to minimal effects of neuropathology. It is known in DS that in comparison to sporadic AD, amyloid accumulation begins earlier in life and there is a longer period of latency between A β neuropathology and overt clinical changes (Wiseman, Al-Janabi et al. 2015). Our results indicate that this latency period is potentially accompanied by some white matter compensatory plasticity which may maintain cognitive ability.

The present study provides evidence of the importance and efficacy of the structural network in predicting AD neuropathology and cognitive performance in DS, however, several limitations must be taken into account. Firstly, despite the unusually large sample size for a DS cohort, support vector techniques benefit from large datasets and therefore generalisability may be somewhat limited. Secondly, consensus diagnoses of AD and MCI were performed for all individuals of the study, revealing a small section of the sample to have either MCI or full AD. These individuals may have added to data heterogeneity, although to provide a realistic analysis of aging individuals with DS, they were retained for the study. The ability of diffusion-weighted data to accurately capture the white matter connectome is also an important methodological factor for consideration. Recent studies demonstrate the importance of whole brain connectomic approaches in understanding cognition in a range of clinical syndromes (Shen, Finn et al. 2017, Kaestner, Balachandra et al. 2020), nevertheless, reproducibility and validity of networks is seldom addressed in the literature. Evidence from test-retest reliability investigation of the structural connectome shows that seeding from the white matter grey matter boundary (Smith, Tournier et al. 2012) and using a two-fibre model with probabilistic rather than deterministic tractography, as performed in the present study methodology, significantly improves test-retest performance (Buchanan, Pernet et al. 2014). Moreover, the white matter connectome has been shown to associate with and affect neuronal avalanches as measured by magnetoencephalography (MEG), evidencing reliable structure-function coupling (Sorrentino, Seguin et al. 2021). Therefore, whilst limitations of diffusion-derived connectomes exist, existing studies support their utility and validity as cognitive and pathological biomarkers.

As the study data was collected at three sites, there is also a potential of inter-site and inter-scanner variability, which may have affected the data homogeneity despite study design and post-processing sameness. Potential inflammatory contribution to diffusion-weighted image changes in DS was also not accounted for, which would be a worthy inclusion for future studies. The effects of tau accumulation were also not assessed in the present analysis, and

therefore there is the potential for a confounding aspect of the mediating effect of tau on neurodegeneration in this DS cohort. As amyloid and tau accumulation exhibit differing trajectories in DS-AD, it is possible that noise arising from tau trajectories may have influenced model performance, especially given that tau is often more closely related to cognitive decline (Zammit, Tudorascu et al. 2021). For PiB⁺ or PiB⁻ status, a case with any region exceeding threshold values was defined as PiB⁺, and therefore there may have been reduced stringency in defining status. However, given that the support vector model was based upon continuous SUVR measures, this should not have significantly impacted model results. Additionally, the MRI-based analyses for this research were cross-sectional, and future longitudinal study will be of significant benefit for examining and fortifying the evidence for the role of white matter changes in DS-AD.

In conclusion, we present findings that show the diffusion-weighted structural connectome and extracted graph theory measures can be used as an effective and non-invasive modality to predict cognitive performance and amyloid burden within the brain. Especially in cases where amyloid deposition may be more pronounced, the utilisation of machine learning tools and structural network may be a useful tool for predicting neuropathology. Moreover, we highlight the directional nature of changes in the white matter in relation to A β plaque formation and working memory, where network disconnection appears to be significant during the development of DS-AD. To build further upon this work, longitudinal assessment of the white matter connectome to examine white matter connectivity as a predictor of AD as it develops in real-time, along with inclusion of tau accumulation trajectories, would be an interesting future direction. Moreover, exploration of machine learning structural connectome predictors in amyloid positive-only cohorts may yield further insight into prognoses of cognitive decline, via additional reduction of sample heterogeneity and more substantial neuropathology.

Funding

The Alzheimer's Biomarkers Consortium – Down Syndrome (ABC-DS) is funded by the National Institute on Aging and the *Eunice Kennedy Shriver* National Institute for Child Health and Human Development (U01 AG051406 and U01 AG051412).

The NIHR Cambridge Biomedical Research Centre (BRC) is a partnership between Cambridge University Hospitals NHS Foundation Trust and the University of Cambridge, funded by the National Institute for Health Research (NIHR). S.S.G.B, E.M., M.G., J.B-W., M.W., E.J., Y.T.H., T.D.F., J.P.C., F.I.A., D.K.M., A.J.H. and S.H.Z. are supported by the NIHR Cambridge Biomedical Research Centre (BRC). The views expressed are those of the author(s) and not necessarily those of the NIHR or the Department of Health and Social Care.

The Alzheimer's Research-UK (AR-UK) (AR-UK-PG2015-23) and Medical Research Council (MRC) (G1002252) also provided funding.

Acknowledgements

This work was supported by researchers at the National Institute for Health Research (NIHR) Cambridge Biomedical Research Centre.

Author contributions

S.S.G.B. carried out all data processing, neuroimage and statistical model analyses. E.M., M.G., J.B-W., M.W., E.J., Y.T.H., T.D.F., J.P.C., F.I.A., D.T., A.C., B.T.C., B.L.H., W.E.K., D.K.M., A.J.H. and S.H.Z. contributed substantially to the study conception and design, drafted and revised the article for important intellectual content and gave final approval of the version to be published.

References

- Bastin, M. E., S. Munoz Maniega, K. J. Ferguson, L. J. Brown, J. M. Wardlaw, A. M. MacLullich and J. D. Clayden (2010). "Quantifying the effects of normal ageing on white matter structure using unsupervised tract shape modelling." Neuroimage **51**(1): 1-10.
- Bazydlo, A., M. Zammit, M. Wu, D. Dean, S. Johnson, D. Tudorascu, A. Cohen, K. Cody, B. Ances, C. Laymon, W. Klunk, S. Zaman, B. Handen, A. Alexander, B. Christian and S. Hartley (2021). "White matter microstructure associations with episodic memory in adults with Down syndrome: a tract-based spatial statistics study." J Neurodev Disord **13**(1): 17.
- Beery K.E., B. N. A. (1989). "Developmental Test of Visual-Motor Integration." Cleveland: Modern Curriculum Press.
- Bloom, G. S. (2014). "Amyloid-beta and tau: the trigger and bullet in Alzheimer disease pathogenesis." JAMA Neurol **71**(4): 505-508.
- Brier, M. R., J. B. Thomas, A. M. Fagan, J. Hassenstab, D. M. Holtzman, T. L. Benzinger, J. C. Morris and B. M. Ances (2014). "Functional connectivity and graph theory in preclinical Alzheimer's disease." Neurobiol Aging **35**(4): 757-768.
- Buchanan, C. R., C. R. Pernet, K. J. Gorgolewski, A. J. Storkey and M. E. Bastin (2014). "Test-retest reliability of structural brain networks from diffusion MRI." Neuroimage **86**: 231-243.
- Buschke, H. (1984). "Cued recall in amnesia." J Clin Neuropsychol **6**(4): 433-440.
- Catani, M. (2019). "The anatomy of the human frontal lobe." Handb Clin Neurol **163**: 95-122.
- Chai, T. D., R. (2014). "Root mean square error (RMSE) or mean absolute error (MAE)?" Geosci. Model Dev. **7**. [10.5194/gmdd-7-1525-2014](https://doi.org/10.5194/gmdd-7-1525-2014).
- Chang, Y. T., J. L. Hsu, S. H. Huang, S. W. Hsu, C. C. Lee and C. C. Chang (2020). "Functional connectome and neuropsychiatric symptom clusters of Alzheimer's disease." J Affect Disord **273**: 48-54.
- Cope, T. E., T. Rittman, R. J. Borchert, P. S. Jones, D. Vatansever, K. Allinson, L. Passamonti, P. Vazquez Rodriguez, W. R. Bevan-Jones, J. T. O'Brien and J. B. Rowe (2018). "Tau burden and the functional connectome in Alzheimer's disease and progressive supranuclear palsy." Brain **141**(2): 550-567.
- Costanzo, M. and C. Zurzolo (2013). "The cell biology of prion-like spread of protein aggregates: mechanisms and implication in neurodegeneration." Biochem J **452**(1): 1-17.
- Davey, J., H. E. Thompson, G. Hallam, T. Karapanagiotidis, C. Murphy, I. De Caso, K. Krieger-Redwood, B. C. Bernhardt, J. Smallwood and E. Jefferies (2016). "Exploring the role of the posterior middle temporal gyrus in semantic cognition: Integration of anterior temporal lobe with executive processes." Neuroimage **137**: 165-177.
- Dell'Acqua, F. and J. D. Tournier (2018). "Modelling white matter with spherical deconvolution: How and why?" NMR Biomed: e3945.
- Drucker, H., Burges, C., Kaufman, L. Smola, A., Vapnik, V. (1997). "Support vector regression machines." Adv Neural Inform Process Syst.

Esralew, L., Janicki, M.P., DiSipio, M., Jokinen, N., Keller, S.M. and Members of the National Task Group Section on Early Detection and Screening (2013). "National Task Group Early Detection Screen for Dementia: Manual." Available from www.aadmd.org/ntg/screening.

Evenhuis, H. M., Kengen, M.M.F., & Eurlings, H.A.L. (2007). "Dementia Questionnaire for People with Learning Disabilities (DLD)." UK adaptation. San Antonia: Harcourt Assessment.

Fenoll, R., J. Pujol, S. Esteba-Castillo, S. de Sola, N. Ribas-Vidal, J. Garcia-Alba, G. Sanchez-Benavides, G. Martinez-Vilavella, J. Deus, M. Dierssen, R. Novell-Alsina and R. de la Torre (2017). "Anomalous White Matter Structure and the Effect of Age in Down Syndrome Patients." J Alzheimers Dis **57**(1): 61-70.

Fornari, S., A. Schafer, M. Jucker, A. Goriely and E. Kuhl (2019). "Prion-like spreading of Alzheimer's disease within the brain's connectome." J R Soc Interface **16**(159): 20190356.

Glantz, S. A., Slinker, B. K. (1990). "Primer of Applied Regression and Analysis of Variance." McGraw-Hill ISBN 978-0-07-023407-9.

Graff-Radford, J., E. M. Arenaza-Urquijo, D. S. Knopman, C. G. Schwarz, R. D. Brown, A. A. Rabinstein, J. L. Gunter, M. L. Senjem, S. A. Przybelski, T. Lesnick, C. Ward, M. M. Mielke, V. J. Lowe, R. C. Petersen, W. K. Kremers, K. Kantarci, C. R. Jack and P. Vemuri (2019). "White matter hyperintensities: relationship to amyloid and tau burden." Brain **142**(8): 2483-2491.

Grill-Spector, K., Z. Kourtzi and N. Kanwisher (2001). "The lateral occipital complex and its role in object recognition." Vision Res **41**(10-11): 1409-1422.

Haxby, J. V. (1989). "Neuropsychological evaluation of adults with Down's syndrome: patterns of selective impairment in non-demented old adults." J Ment Defic Res **33 (Pt 3)**: 193-210.

Head, E., A. M. Helman, D. Powell and F. A. Schmitt (2018). "Down syndrome, beta-amyloid and neuroimaging." Free Radic Biol Med **114**: 102-109.

Huang, S. Y., J. L. Hsu, K. J. Lin and I. T. Hsiao (2020). "A Novel Individual Metabolic Brain Network for 18F-FDG PET Imaging." Front Neurosci **14**: 344.

Kaestner, E., A. R. Balachandra, N. Bahrami, A. Reyes, S. J. Lalani, A. C. Macari, N. L. Voets, D. L. Drane, B. M. Paul, L. Bonilha and C. R. McDonald (2020). "The white matter connectome as an individualized biomarker of language impairment in temporal lobe epilepsy." Neuroimage Clin **25**: 102125.

Kassraian-Fard, P., C. Matthis, J. H. Balsters, M. H. Maathuis and N. Wenderoth (2016). "Promises, Pitfalls, and Basic Guidelines for Applying Machine Learning Classifiers to Psychiatric Imaging Data, with Autism as an Example." Front Psychiatry **7**: 177.

Korbel, J. O., T. Tirosh-Wagner, A. E. Urban, X. N. Chen, M. Kasowski, L. Dai, F. Grubert, C. Erdman, M. C. Gao, K. Lange, E. M. Sobel, G. M. Barlow, A. S. Aylsworth, N. J. Carpenter, R. D. Clark, M. Y. Cohen, E. Doran, T. Falik-Zaccari, S. O. Lewin, I. T. Lott, B. C. McGillivray, J. B. Moeschler, M. J. Pettenati, S. M. Pueschel, K. W. Rao, L. G. Shaffer, M. Shohat, A. J. Van Riper, D. Warburton, S. Weissman, M. B. Gerstein, M. Snyder and J. R. Korenberg (2009). "The genetic architecture of Down syndrome phenotypes revealed by high-resolution analysis of human segmental trisomies." Proc Natl Acad Sci U S A **106**(29): 12031-12036.

Korkman M., K. U., Kemp S.A. (2007). "NEPSY-II." San Antonio, TX: Harcourt Assessment Inc.

Kuang, L., Y. Gao, Z. Chen, J. Xing, F. Xiong and A. X. Han (2020). "White Matter Brain Network Research in Alzheimer's Disease Using Persistent Features." Molecules **25**(11).

Lao, P. J., B. L. Handen, T. J. Betthausen, K. A. Cody, A. D. Cohen, D. L. Tudorascu, C. K. Stone, J. C. Price, S. C. Johnson, W. E. Klunk and B. T. Christian (2019). "Imaging neurodegeneration in Down syndrome: brain templates for amyloid burden and tissue segmentation." Brain Imaging Behav **13**(2): 345-353.

Lee, S., F. Viqar, M. E. Zimmerman, A. Narkhede, G. Tosto, T. L. Benzinger, D. S. Marcus, A. M. Fagan, A. Goate, N. C. Fox, N. J. Cairns, D. M. Holtzman, V. Buckles, B. Ghetti, E. McDade, R. N. Martins, A. J. Saykin, C. L. Masters, J. M. Ringman, N. S. Ryan, S. Forster, C. Laske, P. R. Schofield, R. A. Sperling, S. Salloway, S. Correia, C. Jack, Jr., M. Weiner, R. J. Bateman, J. C. Morris, R. Mayeux, A. M. Brickman and N. Dominantly Inherited Alzheimer (2016). "White matter hyperintensities are a core feature of Alzheimer's disease: Evidence from the dominantly inherited Alzheimer network." Ann Neurol **79**(6): 929-939.

Lin, S. Y., C. P. Lin, T. J. Hsieh, C. F. Lin, S. H. Chen, Y. P. Chao, Y. S. Chen, C. C. Hsu and L. W. Kuo (2019). "Multiparametric graph theoretical analysis reveals altered structural and functional network topology in Alzheimer's disease." Neuroimage Clin **22**: 101680.

Mak, E., A. Bickerton, C. Padilla, M. J. Walpert, T. Annus, L. R. Wilson, Y. T. Hong, T. D. Fryer, J. P. Coles, F. I. Aigbirhio, B. T. Christian, B. L. Handen, W. E. Klunk, D. K. Menon, P. J. Nestor, S. H. Zaman and A. J. Holland (2019). "Longitudinal trajectories of amyloid deposition, cortical thickness, and tau in Down syndrome: A deep-phenotyping case report." Alzheimers Dement (Amst) **11**: 654-658.

Morgan, S. E., J. Seidlitz, K. J. Whitaker, R. Romero-Garcia, N. E. Clifton, C. Scarpazza, T. van Amelsvoort, M. Marcelis, J. van Os, G. Donohoe, D. Mothersill, A. Corvin, A. Pocklington, A. Raznahan, P. McGuire, P. E. Vertes and E. T. Bullmore (2019). "Cortical patterning of abnormal morphometric similarity in psychosis is associated with brain expression of schizophrenia-related genes." Proc Natl Acad Sci U S A **116**(19): 9604-9609.

Moscoso, A., D. Rey-Bretal, J. Silva-Rodriguez, J. M. Aldrey, J. Cortes, J. Pias-Peleteiro, A. Ruibal, P. Aguiar and I. Alzheimer's Disease Neuroimaging (2020). "White matter hyperintensities are associated with subthreshold amyloid accumulation." Neuroimage **218**: 116944.

Neale, N., C. Padilla, L. M. Fonseca, T. Holland and S. Zaman (2018). "Neuroimaging and other modalities to assess Alzheimer's disease in Down syndrome." Neuroimage Clin **17**: 263-271.

Ohlhauser, L., A. F. Parker, C. M. Smart, J. R. Gawryluk and I. Alzheimer's Disease Neuroimaging (2019). "White matter and its relationship with cognition in subjective cognitive decline." Alzheimers Dement (Amst) **11**: 28-35.

Polymenidou, M. and D. W. Cleveland (2012). "Prion-like spread of protein aggregates in neurodegeneration." J Exp Med **209**(5): 889-893.

Powell, D., A. Caban-Holt, G. Jicha, W. Robertson, R. Davis, B. T. Gold, F. A. Schmitt and E. Head (2014). "Frontal white matter integrity in adults with Down syndrome with and without dementia." Neurobiol Aging **35**(7): 1562-1569.

Prasher, V. P., M. J. Farrer, A. M. Kessling, E. M. Fisher, R. J. West, P. C. Barber and A. C. Butler (1998). "Molecular mapping of Alzheimer-type dementia in Down's syndrome." Ann Neurol **43**(3): 380-383.

Rosen, R. F., J. J. Fritz, J. Dooyema, A. F. Cintron, T. Hamaguchi, J. J. Lah, H. LeVine, 3rd, M. Jucker and L. C. Walker (2012). "Exogenous seeding of cerebral beta-amyloid deposition in betaAPP-transgenic rats." J Neurochem **120**(5): 660-666.

Rousset, O. G., Y. Ma and A. C. Evans (1998). "Correction for partial volume effects in PET: principle and validation." J Nucl Med **39**(5): 904-911.

Rubinov, M. and O. Sporns (2010). "Complex network measures of brain connectivity: uses and interpretations." Neuroimage **52**(3): 1059-1069.

S., R. (1994). "Reiss Screen for Maladaptive Behavior." Worthington, OH: International Diagnostic Systems.

Shen, X., E. S. Finn, D. Scheinost, M. D. Rosenberg, M. M. Chun, X. Papademetris and R. T. Constable (2017). "Using connectome-based predictive modeling to predict individual behavior from brain connectivity." Nat Protoc **12**(3): 506-518.

Smith, R. E., J. D. Tournier, F. Calamante and A. Connelly (2012). "Anatomically-constrained tractography: improved diffusion MRI streamlines tractography through effective use of anatomical information." Neuroimage **62**(3): 1924-1938.

Smith, R. E., J. D. Tournier, F. Calamante and A. Connelly (2015). "The effects of SIFT on the reproducibility and biological accuracy of the structural connectome." Neuroimage **104**: 253-265.

Smith, R. E., J. D. Tournier, F. Calamante and A. Connelly (2015). "SIFT2: Enabling dense quantitative assessment of brain white matter connectivity using streamlines tractography." Neuroimage **119**: 338-351.

Sorrentino, P., C. Seguin, R. Rucco, M. Liparoti, E. Troisi Lopez, S. Bonavita, M. Quarantelli, G. Sorrentino, V. Jirsa and A. Zalesky (2021). "The structural connectome constrains fast brain dynamics." Elife **10**.

Tournier J.D., C. F. C. A. (2010). "Improved probabilistic streamlines tractography by 2nd order integration over fibre orientation distributions." Proceedings of the International Society for Magnetic Resonance in Medicine: 1670.

Tournier, J. D., F. Calamante and A. Connelly (2007). "Robust determination of the fibre orientation distribution in diffusion MRI: non-negativity constrained super-resolved spherical deconvolution." Neuroimage **35**(4): 1459-1472.

Tournier, J. D., R. Smith, D. Raffelt, R. Tabbara, T. Dhollander, M. Pietsch, D. Christiaens, B. Jeurissen, C. H. Yeh and A. Connelly (2019). "MRtrix3: A fast, flexible and open software framework for medical image processing and visualisation." Neuroimage **202**: 116137.

Tziortzi, A. C., G. E. Searle, S. Tzimopoulou, C. Salinas, J. D. Beaver, M. Jenkinson, M. Laruelle, E. A. Rabiner and R. N. Gunn (2011). "Imaging dopamine receptors in humans with [11C]-(+)-PHNO: dissection of D3 signal and anatomy." Neuroimage **54**(1): 264-277.

Veitch, D. P., M. W. Weiner, P. S. Aisen, L. A. Beckett, N. J. Cairns, R. C. Green, D. Harvey, C. R. Jack, Jr., W. Jagust, J. C. Morris, R. C. Petersen, A. J. Saykin, L. M. Shaw, A. W. Toga, J. Q. Trojanowski and I. Alzheimer's Disease Neuroimaging (2019). "Understanding disease progression and improving Alzheimer's disease clinical trials: Recent highlights from the Alzheimer's Disease Neuroimaging Initiative." Alzheimers Dement **15**(1): 106-152.

Weaver, N. A., T. Doeven, F. Barkhof, J. M. Biesbroek, O. N. Groeneveld, H. J. Kuijf, N. D. Prins, P. Scheltens, C. E. Teunissen, W. M. van der Flier, G. J. Biessels and T.-V. s. group (2019). "Cerebral amyloid burden is associated with white matter hyperintensity location in specific posterior white matter regions." Neurobiol Aging **84**: 225-234.

Wechsler, D. (2003). "Wechsler intelligence scale for children (4th ed.)." San Antonio, TX: The Psychological Corporation.

Weickenmeier, J., E. Kuhl and A. Goriely (2018). "Multiphysics of Prionlike Diseases: Progression and Atrophy." Phys Rev Lett **121**(15): 158101.

Wiseman, F. K., T. Al-Janabi, J. Hardy, A. Karmiloff-Smith, D. Nizetic, V. L. Tybulewicz, E. M. Fisher and A. Strydom (2015). "A genetic cause of Alzheimer disease: mechanistic insights from Down syndrome." Nat Rev Neurosci **16**(9): 564-574.

Xu, Y. and R. Goodacre (2018). "On Splitting Training and Validation Set: A Comparative Study of Cross-Validation, Bootstrap and Systematic Sampling for Estimating the Generalization Performance of Supervised Learning." J Anal Test **2**(3): 249-262.

Ye, C., S. Mori, P. Chan and T. Ma (2019). "Connectome-wide network analysis of white matter connectivity in Alzheimer's disease." Neuroimage Clin **22**: 101690.

Zacharaki, E. I., S. Wang, S. Chawla, D. Soo Yoo, R. Wolf, E. R. Melhem and C. Davatzikos (2009). "Classification of brain tumor type and grade using MRI texture and shape in a machine learning scheme." Magn Reson Med **62**(6): 1609-1618.

Zammit, M. D., C. M. Laymon, T. J. Betthausen, K. A. Cody, D. L. Tudorascu, D. S. Minhas, M. N. Sabbagh, S. C. Johnson, S. H. Zaman, C. A. Mathis, W. E. Klunk, B. L. Handen, A. D. Cohen and B. T. Christian (2020). "Amyloid accumulation in Down syndrome measured with amyloid load." Alzheimers Dement (Amst) **12**(1): e12020.

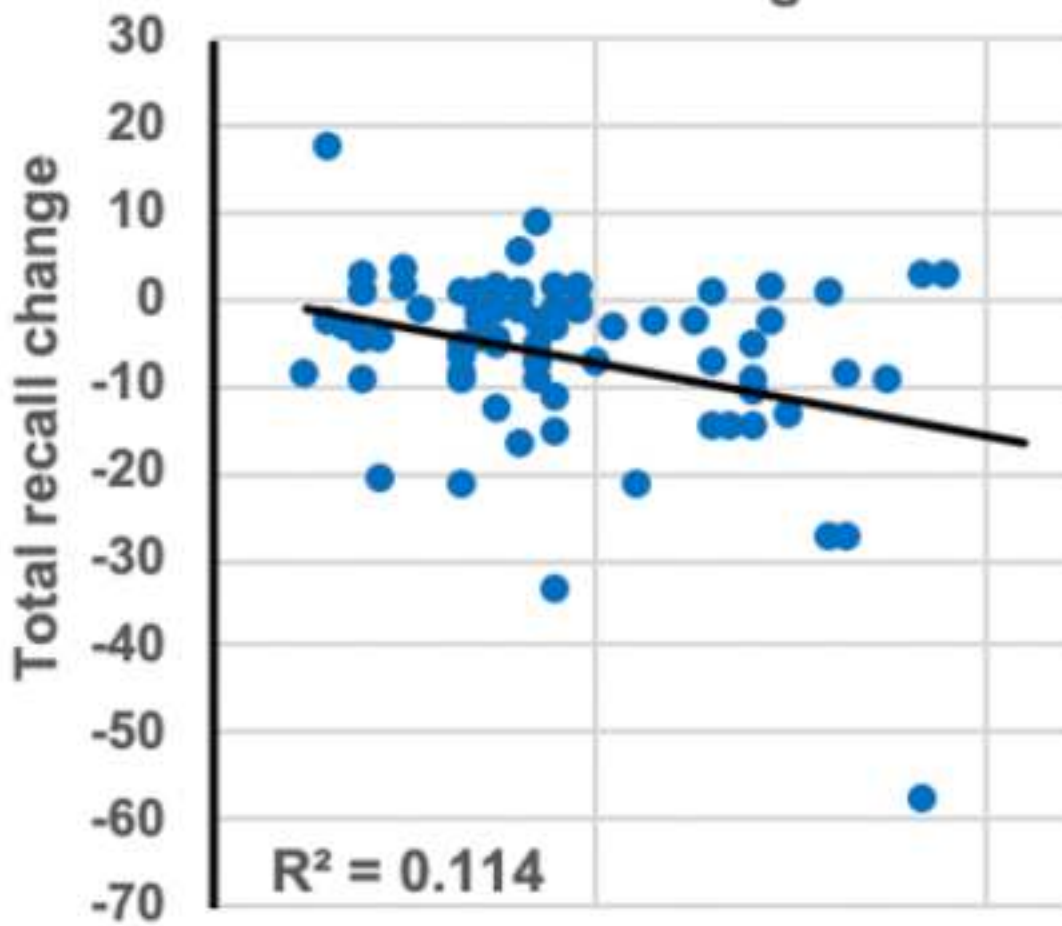
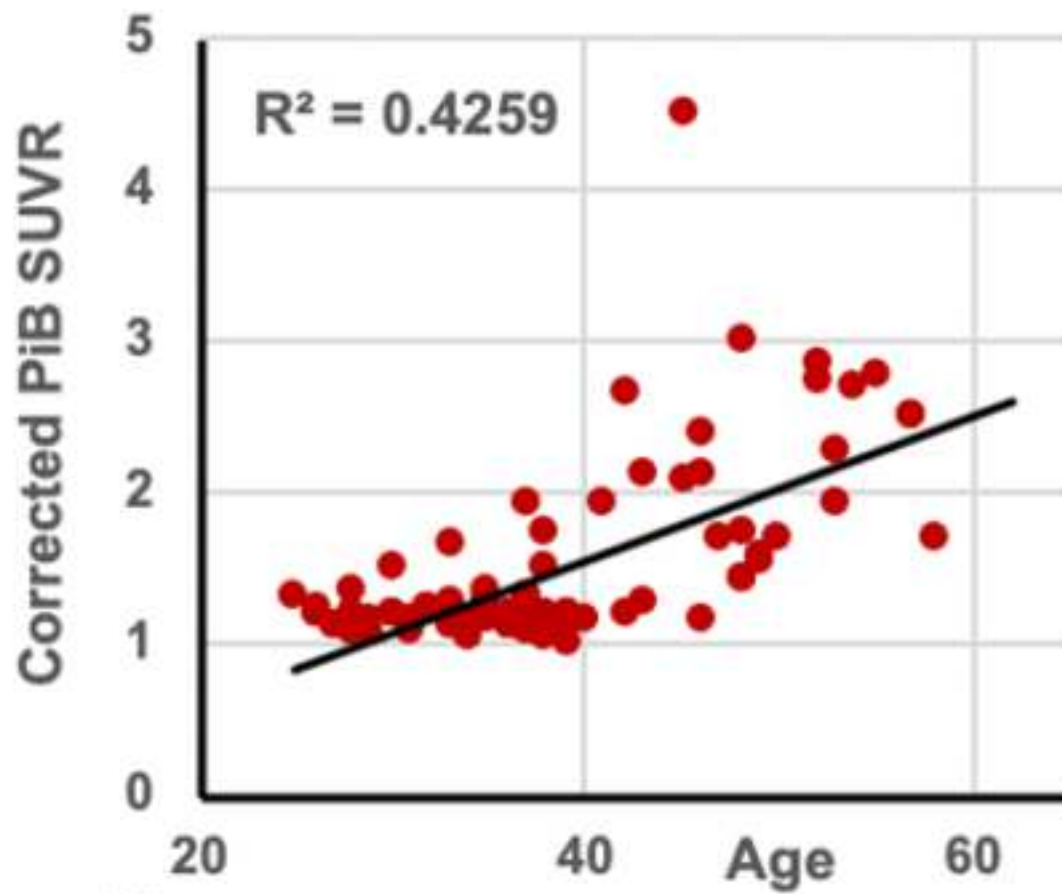
Zammit, M. D., D. L. Tudorascu, C. M. Laymon, S. L. Hartley, P. A. Ellison, S. H. Zaman, B. M. Ances, S. C. Johnson, C. K. Stone, M. N. Sabbagh, C. A. Mathis, W. E. Klunk, A. D. Cohen, B. L. Handen and B. T. Christian (2021). "Neurofibrillary tau depositions emerge with subthreshold cerebral beta-amyloidosis in down syndrome." Neuroimage Clin **31**: 102740.

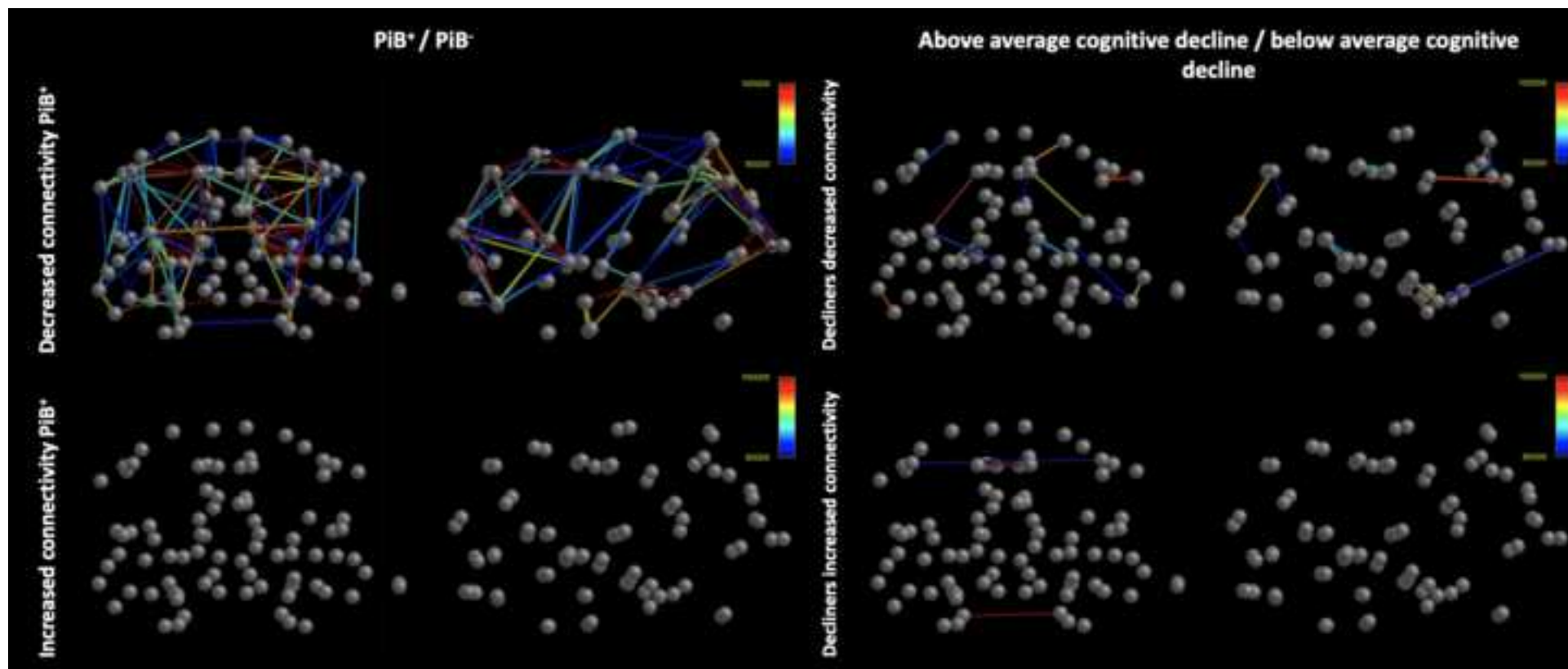
Zhu, D., K. Li, D. P. Terry, A. N. Puente, L. Wang, D. Shen, L. S. Miller and T. Liu (2014). "Connectome-scale assessments of structural and functional connectivity in MCI." Hum Brain Mapp **35**(7): 2911-2923.

Figure 1. Higher corrected PiB SUVR values (global, as defined by average of regions of interest) and worse longitudinal cognitive decline (as measured by the total recall task) are significantly associated with increasing age ($p < 0.001$ and $p < 0.01$ respectively).

Figure 2. Structural connectome representation of the differences between mean white matter connection density for the PiB⁺ group compared to the PiB⁻ group and the above average cognitive decline group compared to the below average cognitive decline group, as evidenced by rank-based feature selection. Node-to-node connectivity thresholded at 50,000 streamlines. Colour bars reference degree of connection density for edges, and node colours are random for each structurally defined brain region.

Figure 3. Features selected ($p < 0.01$) from graph theory metrics based on rank-based differences between the PiB⁺ and PiB⁻ groups. Mean node strength (sum of connection density weights connected to the node) and mean node degree of selected features as separated by group, exhibiting uniform lower node strength and degree for the PiB⁺ group compared to the PiB⁻ group.





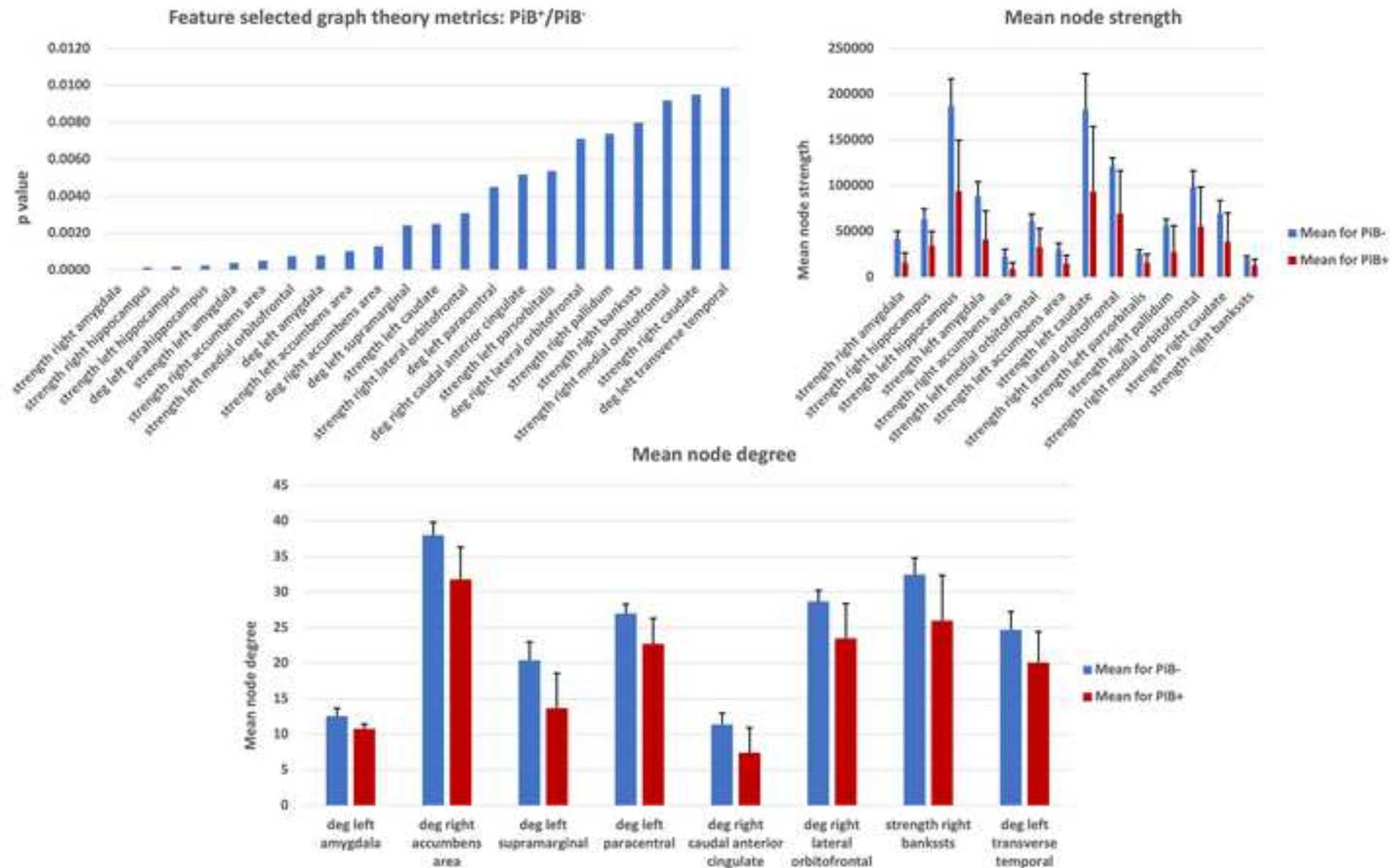


Table 1. Participant demographics		
	PiB⁺	PiB⁻
n	35	60
Age (mean / SD)	46.7 / 8.0	34.4 / 5.2
Sex (m / f)	24 / 11	32 / 28
Data acquired for baseline cognition (%)	91.4	96.7
Data acquired for month 16 cognition (%)	80.0	80.0
Cued Recall Total baseline (mean / SD)	21.8 / 15.5	30.8 / 6.3
Longitudinal change in Cued Recall Total (mean / SD)	-9.4 / 8.5	-2.7 / 11.6
Diagnostic consensus MCI	3	1
Diagnostic consensus dementia	3	0
Diagnostic consensus unable to determine	1	1

Table 1. Participant demographics for the complete Down's syndrome sample.

Table 2. Linear kernel support vector machine model performance											
Predictors: Structural network connectivity				Predictors: Graph theory network metrics				Predictors: Age-only			
Response variable	Global PiB SUVR	Recall baseline*	Recall change	Response variable	Global PiB SUVR*	Recall baseline	Recall change	Response variable	Global PiB SUVR	Recall baseline	Recall change*
RMSE	0.43	8.56	10.42	RMSE	0.40	No features selected ($p < 0.01$)		RMSE	0.41	10.36	9.80
R²	0.15	0.34	0.08	R²	0.28			R²	0.28	0.03	0.17
MSE	0.19	73.42	108.47	MSE	0.16			MSE	0.16	107.34	96.07
MAE	0.27	5.58	7.10	MAE	0.26			MAE	0.26	6.71	6.41

Table 2. SVM model performance with the structural network, graph theory network and age as predictive metrics, as measured by root mean square error (RMSE), R^2 , mean square error (MSE) and mean absolute error (MAE).

Neurobiology of Aging Response to Reviewer's Comments

"Support vector machine learning and diffusion-derived structural networks predict amyloid quantity and cognition in adults with Down's syndrome"

Editors' comments:

Please consider our reviewer's remaining suggestions for possible improvement as you make any final adjustments in preparation for publication.

Thank you for submitting this interesting work to Neurobiology of Aging.

Response: The authors would like to thank the editor for their provisional acceptance of the manuscript pending minor revision. We have addressed each of the reviewers final points below.

Reviewers' comments:

Reviewer #3: I appreciate that the authors appear to have responded to my previous comments from the initial review. In particular, they have included discussion of the limitations to the study, with particular attention to the capabilities of diffusion MRI.

Response: The authors thank the reviewer for their time reviewing the manuscript and their additional comments.

I would disagree with their comment that data cleaning processes ("such as denoising, bias correction, and visual quality inspection") minimise the effects of site variability - while these are useful for minimising sources of error within a homogeneous data set, multi-site data would require data harmonisation methods. Would recommend the sentence be removed.

Response: The sentence "However, data cleaning processes such as de-noising, bias correction and visual quality inspection should have minimised these effects." has been removed from the limitations section of the discussion.

The additional detail provided in the Figure legends is valuable; however, I still find it very difficult to decipher Figure 2. The colour scale does not meaningfully separate connection density for different edges - perhaps the authors could consider using a tighter threshold, a different colour scale, or use line thickness to distinguish connection density? Providing random node colours is also quite confusing - perhaps only the relevant nodes need be presented, and overlaid on anatomy for easier interpretation?

Response: The authors thank the reviewer for the suggestions to improve Figure 2. For each figure subsection (Decreased connectivity PiB⁺, Increased connectivity PiB⁺, [cognitive] Decliners decreased connectivity and [cognitive] Decliners increased connectivity), the threshold has been tightened to more evenly spread the data along the colour scale. In addition, the colour scale has been changed to blue-green-yellow-red, so as to more meaningfully separate connection density extent. To minimise confusion from random node colouring, all nodes have been changed to grey. Overlay on anatomy has not been included, as the connectome is a 3-dimensional image and therefore the authors feel that overlay on a 2-dimensional image would be visually misleading.

Verification

The co-authors approve this manuscript and I can certify that this manuscript is not under review at any other publication. The work contained within this manuscript does not overlap with any other submissions or reports and conflicts are appropriately reported in the manuscript.

TRIPOD Checklist: Prediction Model Development and Validation

Section/Topic	Item	Checklist Item	Page	
Title and abstract				
Title	1	D;V	Identify the study as developing and/or validating a multivariable prediction model, the target population, and the outcome to be predicted.	1
Abstract	2	D;V	Provide a summary of objectives, study design, setting, participants, sample size, predictors, outcome, statistical analysis, results, and conclusions.	1
Introduction				
Background and objectives	3a	D;V	Explain the medical context (including whether diagnostic or prognostic) and rationale for developing or validating the multivariable prediction model, including references to existing models.	1-2
	3b	D;V	Specify the objectives, including whether the study describes the development or validation of the model or both.	2
Methods				
Source of data	4a	D;V	Describe the study design or source of data (e.g., randomized trial, cohort, or registry data), separately for the development and validation data sets, if applicable.	3
	4b	D;V	Specify the key study dates, including start of accrual; end of accrual; and, if applicable, end of follow-up.	3
Participants	5a	D;V	Specify key elements of the study setting (e.g., primary care, secondary care, general population) including number and location of centres.	3
	5b	D;V	Describe eligibility criteria for participants.	3
	5c	D;V	Give details of treatments received, if relevant.	N/A
Outcome	6a	D;V	Clearly define the outcome that is predicted by the prediction model, including how and when assessed.	6
	6b	D;V	Report any actions to blind assessment of the outcome to be predicted.	N/A
Predictors	7a	D;V	Clearly define all predictors used in developing or validating the multivariable prediction model, including how and when they were measured.	4
	7b	D;V	Report any actions to blind assessment of predictors for the outcome and other predictors.	N/A
Sample size	8	D;V	Explain how the study size was arrived at.	3
Missing data	9	D;V	Describe how missing data were handled (e.g., complete-case analysis, single imputation, multiple imputation) with details of any imputation method.	6
Statistical analysis methods	10a	D	Describe how predictors were handled in the analyses.	5-6
	10b	D	Specify type of model, all model-building procedures (including any predictor selection), and method for internal validation.	5-6
	10c	V	For validation, describe how the predictions were calculated.	6
	10d	D;V	Specify all measures used to assess model performance and, if relevant, to compare multiple models.	5-6
	10e	V	Describe any model updating (e.g., recalibration) arising from the validation, if done.	N/A
Risk groups	11	D;V	Provide details on how risk groups were created, if done.	N/A
Development vs. validation	12	V	For validation, identify any differences from the development data in setting, eligibility criteria, outcome, and predictors.	6
Results				
Participants	13a	D;V	Describe the flow of participants through the study, including the number of participants with and without the outcome and, if applicable, a summary of the follow-up time. A diagram may be helpful.	6
	13b	D;V	Describe the characteristics of the participants (basic demographics, clinical features, available predictors), including the number of participants with missing data for predictors and outcome.	6, Table 1
	13c	V	For validation, show a comparison with the development data of the distribution of important variables (demographics, predictors and outcome).	5-6
Model development	14a	D	Specify the number of participants and outcome events in each analysis.	Table 1
	14b	D	If done, report the unadjusted association between each candidate predictor and outcome.	6, Figure 1
Model specification	15a	D	Present the full prediction model to allow predictions for individuals (i.e., all regression coefficients, and model intercept or baseline survival at a given time point).	6-7
	15b	D	Explain how to use the prediction model.	6-7
Model performance	16	D;V	Report performance measures (with CIs) for the prediction model.	7, Table 2
Model-updating	17	V	If done, report the results from any model updating (i.e., model specification, model performance).	N/A
Discussion				
Limitations	18	D;V	Discuss any limitations of the study (such as nonrepresentative sample, few events per predictor, missing data).	10
Interpretation	19a	V	For validation, discuss the results with reference to performance in the development data, and any other validation data.	8-10
	19b	D;V	Give an overall interpretation of the results, considering objectives, limitations, results from similar studies, and other relevant evidence.	8-10
Implications	20	D;V	Discuss the potential clinical use of the model and implications for future research.	8-10
Other information				
Supplementary information	21	D;V	Provide information about the availability of supplementary resources, such as study protocol, Web calculator, and data sets.	N/A
Funding	22	D;V	Give the source of funding and the role of the funders for the present study.	10

*Items relevant only to the development of a prediction model are denoted by D, items relating solely to a validation of a prediction model are denoted by V, and items relating to both are denoted D;V. We recommend using the TRIPOD Checklist in conjunction with the TRIPOD Explanation and Elaboration document.